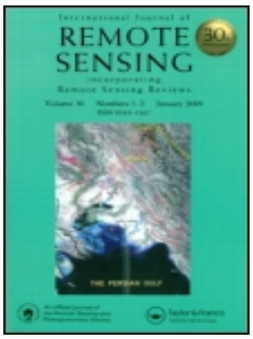

International Journal of Remote Sensing

ISSN: 0143-1161 (Print) 1366-5901 (Online) Journal homepage: www.tandfonline.com/journals/tres20

An improved method of night-time light saturation reduction based on EVI

Li Zhuo, Jing Zheng, Xiaofan Zhang, Jun Li & Lin Liu

To cite this article: Li Zhuo, Jing Zheng, Xiaofan Zhang, Jun Li & Lin Liu (2015) An improved method of night-time light saturation reduction based on EVI, International Journal of Remote Sensing, 36:16, 4114-4130, DOI: 10.1080/01431161.2015.1073861

To link to this article: https://doi.org/10.1080/01431161.2015.1073861

International Journal of Remote Sensing, 2015
Vol. 36, No. 16, 4114–4130, http://dx.doi.org/10.1080/01431161.2015.1073861

Taylor & Francis
Taylor & Francis Group

An improved method of night-time light saturation reduction based on EVI

Li Zhuo[a]*, Jing Zheng[b], Xiaofan Zhang[a], Jun Li[a], and Lin Liu[a]

[a]*Guangdong Provincial Key Laboratory of Urbanization and Geo-simulation, School of Geography and Planning, Sun Yat-sen University, Guangzhou 510275, PR China;* [b]*Guangdong Climate Centre, Guangzhou 510080, PR China*

(*Received 7 February 2015; accepted 13 July 2015*)

Defense Meteorological Satellite Program (DMSP) Operational Linescan System (OLS) night-time light (NTL) data have been widely applied to studies on anthropogenic activities and their interactions with the environment. Due to limitations of the OLS sensor, DMSP NTL data suffer from a saturation problem in central urban areas, which further affects studies based on nocturnal lights. Recently, the vegetation-adjusted NTL urban index (VANUI) has been developed based on the inverse correlation of vegetation and urban surfaces. Despite its simple implementation and ability to effectively increase variations in NTL data, VANUI does not perform well in certain rapidly growing cities. In this study, we propose a new index, denoted enhanced vegetation index (EVI)-adjusted NTL index (EANTLI), that was developed by reforming the VANUI algorithm and utilizing the EVI. Comparisons with radiance-calibrated NTL (RCNTL) and the new Visible Infrared Imager Radiometer Suite (VIIRS) data for 15 cities worldwide show that EANTLI reduces saturation in urban cores and mitigates the blooming effect in suburban areas. EANTLI's similarity to RCNTL and VIIRS is consistently higher than VANUI's similarity to RCNTL and VIIRS in both spatial distribution and latitudinal transects. EANTLI also yields better results in the estimation of electric power consumption of 166 Chinese prefecture-level cities. In conclusion, EANTLI can effectively reduce NTL saturation in urban centres, thus presenting great potential for wide-range applications.

1. Introduction

In contrast to the Landsat Thematic Mapper (TM), Système Pour l'Observation de la Terre (SPOT) High Resolution Visible (HRV) or National Oceanic and Atmospheric Administration (NOAA) Advanced Very High Resolution Radiometer (AVHRR) sensors, which record reflectance from the Earth's surface in the daytime, the Defense Meteorological Satellite Program (DMSP) Operational Linescan System (OLS) has a unique capability of detecting night-time lights (NTLs). Although it was originally designed to detect the global distribution of clouds and cloud top temperatures, researchers found that the visible and near-infrared (VNIR) band from this sensor had the potential to observe a series of faint VNIR emission sources, such as city lights, aurorae, gas flares, and fires. In 1992, the National Geophysical Data Center (NGDC) at NOAA established digital archives of the DMSP-OLS night-time light data (Elvidge et al. 1999). Different data sets, such as time-series 'stable light' data and radiance-calibrated data, have been developed since the establishment of the archives. These data sets have been applied to

*Corresponding author. Email: zhuoli@mail.sysu.edu.cn

monitor and analyse human activities and natural phenomena, such as urbanization (Lo 2002; Ma et al. 2012; Pandey, Joshi, and Seto 2013; Sutton 2003; Wei et al. 2014; Zhang and Seto 2011) and its effects on the ecosystem (Imhoff et al. 2000, 2004), estimation of urban populations (Amaral et al. 2005, 2006; Elvidge et al. 1997; Lo 2001; Raupach, Rayner, and Paget 2010; Zeng et al. 2011; Zhuo et al. 2009), socio-economic activities (Chen and Nordhaus 2011; Elvidge et al. 1997, 2012; Ghosh et al. 2010; Henderson, Storeygard, and Weil 2012; Sutton, Elvidge, and Ghosh 2007), energy consumption (Chalkias et al. 2006; Chand et al. 2009; Elvidge et al. 1997; He et al. 2012), and greenhouse gas emission (Doll, Muller, and Elvidge 2000; Letu, Nakajima, and Nishio 2014; Raupach, Rayner, and Paget 2010).

Despite its unique features and advantages, the OLS sensor also has shortcomings (Elvidge et al. 2007), including the following: (1) coarse spatial resolution; (2) lack of on-board calibration; (3) lack of in-flight gain change records; (4) 6-bit quantization and limited dynamic range; (5) light saturation in urban centres in the standard high-gain-setting operation; and (6) the 'blooming' effect due to the coarse spatial resolution, the accumulation of geolocation errors, and the detection of diffuse and scattered light. Among these shortcomings, the light saturation problem and the 'blooming' effect are the two largest obstacles in applications of the time-series data set. Saturation in urban centres conceals light intensity variations and spatial details, while the 'blooming' effect leads to the overestimation of the lighted area. Therefore, methods to correct or reduce NTL saturation have been a popular topic in NTL studies.

To partially address the signal saturation in urban centres and the lack of on-board calibration, the NGDC developed a strategy to collect fixed gain data at low, medium, and high gain settings and convert them to 'radiance' based on the preflight calibration available for each of the OLS sensors. These special data collections have been occasionally requested and received by the NGDC since 1996. In 1999, Elvidge et al. (1999) produced a radiance-calibrated night-time light image of the USA using the mentioned data collections. Following a similar scheme, Ziskin, Baugh, and Hsu (2010) produced a global night-time light product of 2006 with no sensor saturation in 2010 by combining the data acquired at low gain settings with the operational data acquired at high gain settings. The radiance-calibrated data successfully solve the light saturation problem in urban areas, and empirical studies have proved that it is a useful spatial indicator for energy-related human activities. However, the radiance-calibrated data sets are only available for a limited number of years because the OLS data at fixed gain settings could only be requested and generated during the new moon stages of certain lunar cycles.

Researchers also developed other methods to overcome the saturation problem in urban centres. Lo (2001) developed a three-dimensional model to extract light volume using the triangulated irregular network functionality in the ArcGIS software. Raupach, Rayner, and Paget (2010) amplified the saturated light data based on a hypothesis of a power-law distribution of light density. Letu et al. (2012) used the 1996–1997 radiance-calibrated data, the 1999 stable light data, and the regression method to generate saturation-corrected data in 1999. Researchers introduced other information, such as vegetation, to reduce saturation effects in urban cores. For example, Zhang, Schaaf, and Seto (2013) proposed the vegetation-adjusted NTL urban index (VANUI) by combining night-time data with the Moderate Resolution Imaging Spectroradiometer (MODIS) normalized difference vegetation index (NDVI). The index is simple to implement and capable of highlighting intra-urban variability in light intensity. However, the index does not perform well in cities that have experienced rapid urbanization, such as Beijing, Chennai, and

Bengaluru. Meanwhile, VANUI still suffers from the blooming effect of the DMSP-OLS NTL data.

On 28 October 2011, the Suomi National Polar-Orbiting Partnership (Suomi NPP) satellite was launched, and the on-board Visible Infrared Imaging Radiometer Suite (VIIRS) sensor began collecting data in the day/night bands (DNBs; Miller et al. 2012). In early 2013, the Earth Observation Group, NOAA/NGDC, released the NPP-VIIRS night-time light data (Baugh et al. 2013; Elvidge et al. 2013; Hillger et al. 2013). This new generation of night-time products resolves many shortcomings of the DMSP-OLS, such as the saturation of urban centres and the lack of on-board calibration. Researchers have proved the great potential of NPP-VIIRS data in estimating socio-economic activities (Li et al. 2013; Shi et al. 2014; Yu et al. 2015). However, data-processing methods of the VIIRS night-time images are not well established, and the data sets do not meet the long-term time-series requirements of certain studies. DMSP-OLS night-time light images remain the dominant source of night-time light observations. Therefore, studies on reducing light saturation of the DMSP-OLS time-series data are needed.

In this study, we propose a new method based on the integration of NTL and the MODIS enhanced vegetation index (EVI). The proposed method is designed to enlarge the original NTL digital number (DN) values inside the potential saturated area (PSA) and reduce those outside the PSA to correct the light saturation in urban cores and mitigate the 'blooming' effect.

2. Data and methods

2.1. Data source

The data used in this study include the version 4 DMSP-OLS night-time lights time-series data set, the global radiance-calibrated night-time lights data set, the first global NPP-VIIRS night-time light data, and the MODIS MCD43D and MOD13A3 products.

The version 4 DMSP-OLS night-time lights time-series data set contains cloud-free annual composites from 1992 to 2013. This data set was constructed by compositing orbital sections that met a stringent set of criteria, namely: (1) centre half of orbital swath; (2) no sunlight present; (3) no moonlight present; (4) no solar glare contamination; (5) cloud-free; and (6) no contamination from auroral emissions. Night-time image data from individual orbits that met these criteria were added into a global latitude–longitude grid (Plate Carree projection) with a resolution of 30 arc seconds (approximately 1 km at the equator). The version 4 data set consists of three types of data: cloud-free coverage, a raw average visible band with no further filtering, and an average visible band of stable lights (i.e. lights from cities, towns, and other sites with persistent lighting). The data of the average visible band of stable lights were used in this study.

The global radiance-calibrated night-time lights data set was produced by merging DMSP-OLS data acquired at low gain settings with operational data acquired at high gain settings. The radiance-calibrated product fixed the gain setting of the DMSP satellite into three stages to record night-time lights of different strengths of brightness. Typically, the highest gain is approximately 100 times more sensitive than the lowest gain. By merging the images obtained under each gain setting, an extra-large dynamic range that can fully accommodate bright city lights is achieved. These fixed-gain images were further blended with the operational stable light product to recover more details in dim areas.

The first global cloud-free composite of NPP-VIIRS night-time lights was generated using VIIRS DNB data collected in nights with no moonlight. Observations made on 18 April 2012 to 26 April 2012 and 11 October 2012 to 23 October 2012 were used. Cloud screening was performed based on the detection of clouds in the VIIRS M15 thermal band. In contrast to the DMSP-OLS data, light detection associated with fires, gas flares, volcanoes or aurora, as well as the background noise were not removed in the VIIRS product. The VIIRS DNB data have substantially lower detection limits than DMSP. The VIIRS data have a spatial resolution of 15 arc second grids (approximately 500 m at the equator; Miller et al. 2012).

The annual mean NDVI values used for calculation of VANUI were obtained following the procedure described in the literature (Zhang, Schaaf, and Seto 2013), which utilizes nadir bidirectional reflectance distribution function (BRFD)-adjusted reflectances (NBAR) derived from MODIS MCD43D products to generate an NBAR-NDVI time series and to calculate annual mean NDVI values from the time-series data.

The EVI data used in this study were derived from the MODIS MOD13A3 product, which contains monthly vegetation index maps at a 1 km spatial resolution. The strict procedure for the generation of composited EVI is listed as follows based on the priority: (1) BRDF composition; (2) maximum value composition in a limited view angle; (3) direct calculation; and (4) maximum value composition (Huete, Justice, and Van Leeuwen 1999).

Because the only available VIIRS night-time light data were observed in 2012, we used the DMSP-OLS time-series data and MODIS MCD43D/ MOD13A3 products of the same year. However, there were no radiance-calibrated night-time light data for 2012; thus, we used the 2010 product, which included observations from 11 January 2010 to 31 July 2011. The time-series and radiance-calibrated night-time light data as well as the VIIRS data were obtained from the NOAA/NGDC Earth Observation Group's website (http://ngdc.noaa.gov/eog/index.html). MODIS MCD43D/MOD13A3 products were downloaded from the MODIS website (http://modis.gsfc.nasa.gov/data/).

2.2. *EVI-adjusted night-time light index (EANTLI)*

In Zhang et al.'s (2013) study, VANUI is developed based on the rationale that key urban features are inversely correlated with vegetation health and abundance. VANUI is defined as in Equation (1):

$$\mathrm{VANUI} = (1 - (\mathrm{NDVI}))(\mathrm{NTL}), \tag{1}$$

where NDVI is the NDVI derived from MODIS. As negative MODIS NDVI values are usually associated with water and glacier, pixels with negative NDVI values are excluded from calculation and a VANUI value of zero is directly assigned. The parenthetical expression '(1 – (NDVI))' inverts the shape of NDVI transects. The native NTL values in the range of [0, 63] are normalized to the range of [0.0, 1.0] to match MODIS NDVI.

VANUI is intuitive and simple to implement, but its performance is limited in cities undergoing rapid development, such as Beijing, Chennai, and Bengaluru (Zhang, Schaaf, and Seto 2013). This limitation is most likely caused by the slight variation in vegetation cover or composition in these cities; thus, the expression of '(1 – (NDVI))' may fail to capture the peaks of night-time lights.

Because NTL is one of the defining urban features, the inverse correlation between NTL and the vegetation index can be observed in most cities, including those undergoing

rapid development; therefore, a new NTL correction method could be developed based on this fact. Considering that NDVI is susceptible to large sources of error and uncertainty under variable atmospheric and canopy background conditions (Liu and Huete 1995), we used EVI in this study, which is calculated using Equation (2):

$$\mathrm{EVI} = G\frac{\rho_{\mathrm{nir}} - \rho_{\mathrm{red}}}{\rho_{\mathrm{nir}} + C_1\rho_{\mathrm{red}} - C_2\rho_{\mathrm{blue}} + L}, \tag{2}$$

where ρ_{nir}, ρ_{red}, and ρ_{blue} are the surface reflectance in the near-infrared, red, and blue bands, respectively. L is the canopy background adjustment that addresses nonlinear, differential near-infrared and red radiant transfer through a canopy, and C_1 and C_2 are the coefficients of the aerosol resistance term. The coefficients adopted in the EVI algorithm are $L = 1$, $C_1 = 6$, $C_2 = 7.5$, and G (gain factor) = 2.5 (Huete et al. 2002).

The inverse relationship between NTL and the vegetation index is then represented by the difference between normalized NTL (denoted as $(\mathrm{NTL})_{\mathrm{norm}}$ in the following text and equations) and EVI (both are in the range of [0, 1]), which decreases with the distance to an urban centre. Based on this pattern and the fact that saturation is less likely to appear when $(\mathrm{NTL})_{\mathrm{norm}}$ is equal to or less than EVI, we use 1 as the NTL's adjustment factor when $(\mathrm{NTL})_{\mathrm{norm}}$ equals EVI as a benchmark. When $(\mathrm{NTL})_{\mathrm{norm}}$ is greater than EVI, the adjustment factor is greater than 1 to restore the response of the OLS sensor to high-intensity lights. In this case, NTL saturation in PSA can be corrected. When $(\mathrm{NTL})_{\mathrm{norm}}$ is less than EVI, the factor is less than 1 to enhance light intensity differences between urban centres and suburban regions, which can be expressed mathematically in Equation (3):

$$\mathrm{EANTLI} = \frac{1 + \left((\mathrm{NTL})_{\mathrm{norm}} - (\mathrm{EVI})\right)}{1 - \left((\mathrm{NTL})_{\mathrm{norm}} - (\mathrm{EVI})\right)}(\mathrm{NTL}), \tag{3}$$

where EANTLI represents the EVI-adjusted NTL index, $(\mathrm{NTL})_{\mathrm{norm}}$ represents normalized NTL, (NTL) is the original NTL value, and (EVI) is the EVI derived from MODIS.

To further analyse EANTLI's rationality, we replace '$((\mathrm{NTL})_{\mathrm{norm}} - (\mathrm{EVI}))$' with d, and Equation (3) can be rewritten as

$$\mathrm{EANTLI} = \left(\frac{2}{1-d} - 1\right)(\mathrm{NTL}). \tag{4}$$

We define the adjustment factor k as in Equation (5):

$$k = \left(\frac{2}{1-d} - 1\right). \tag{5}$$

Then, Equation (3) can be simplified to Equation (6):

$$\mathrm{EANTLI} = k(\mathrm{NTL}). \tag{6}$$

Monotonic analysis shows that k is a monotonically increasing function over the interval of $[-1.0, 1.0]$. Thus, the adjustment factor k increases as d increases. In central urban areas, where the $(\mathrm{NTL})_{\mathrm{norm}}$ values are typically greater than the (EVI) values, d is in the range of [0.0, 1.0], and the adjustment factor k is greater than 1, indicating that the

original NTL DN value will be amplified. In the PSA, in which $(\mathrm{NTL})_{\mathrm{norm}}$ is equal to 1, Equation (3) can be rewritten as follows:

$$\mathrm{EANTLI} = \left(\frac{2}{(\mathrm{EVI})} - 1\right)(\mathrm{NTL}). \tag{7}$$

Therefore, the adjustment factor k is completely determined by (EVI), thus allowing introduction of spatial inhomogeneity inside the PSA. However, if the (EVI) value is equal to 0, then the adjustment factor k becomes infinite. To avoid this unfavourable situation, pixels with an (EVI) value less than 0.01 are excluded from the calculation of EANTLI. In the suburban area, in which $(\mathrm{NTL})_{\mathrm{norm}}$ values are typically less than the (EVI) values, d is in the range of [−1.0, 0.0) and the adjustment factor k will be less than 1, indicating that the original NTL DN values will be reduced.

To illustrate the effectiveness of the adjustment factor k, we selected a latitudinal transect across the Jingjintang (Beijing–Tianjin–Tangshan) Urban Group, plotted DN values of NTL and radiance-calibrated NTL (RCNTL), and calculated values of k along the transect (this figure closely follows Figure 2 of Zhang, Schaaf, and Seto (2013)).

For comparison, we defined two additional adjustment factors, k_1 and k_2, which are described in Equations (8) and (9), respectively:

$$k_1 = \frac{1 + \left((\mathrm{NTL})_{\mathrm{norm}} - (\mathrm{NDVI})\right)}{1 - \left((\mathrm{NTL})_{\mathrm{norm}} - (\mathrm{NDVI})\right)}, \tag{8}$$

$$k_2 = 10(1 - (\mathrm{NDVI})). \tag{9}$$

In Equation (9), the parenthetical expression '(1 – (NDVI))' is multiplied by 10 to match the ranges of k and k_1.

The values of k_1 and k_2 along the transect were also calculated and then plotted in Figure 1. Figure 1 reveals that k_2 shows only a slight variation and fails to capture the peaks of RCNTL data. The k_1 curve shows greater variation; however, it tends to underestimate the peaks in a central urban area. The curve of k best illustrates the inverse relationship between NTL and vegetation, with higher values in the urban core and lower values in the suburban region, which most closely resembles the RCNTL curve (Figure 1).

3. Analysis and evaluation of EANTLI

To fully evaluate the proposed EANTLI, we analysed it from three different angles. First, EANTLI's capability of characterizing intra-urban variability was analysed by comparing its spatial distribution with RCNTL, VIIRS, and VANUI. Second, EANTLI's closeness to RCNTL and VIIRS was assessed using randomly selected latitudinal transects across different cities. Finally, EANTLI's accuracy in estimating electric power consumption was evaluated.

The VIIRS data do not have the issue of oversaturation, thanks to the wide radiometric detection range of the DNB radiometer. The on-board calibration also increases the data quality. Therefore, the VIIRS data are used as 'ground truth' in this section. As suggested by the NGDC, the RCNTL product should be deemed to be unitless due to lack of an on-board calibration system for all DMSP-OLS. But, since it was the best solution for

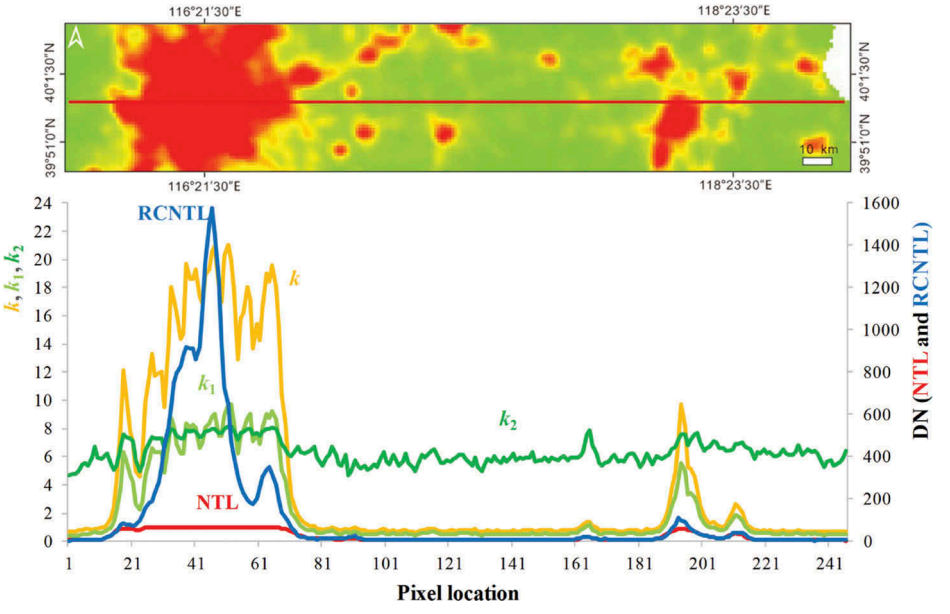

Figure 1. Latitudinal transects of NTL (red), RCNTL (blue), adjustment factor k (orange), k_1 (light green), and k_2 (dark green) across the Jingjintang Urban Group in China.

DMSP-OLS NTL data's saturation problem before VIIRS, we also used it as a reference in this study.

3.1. *Intra-urban variability characterization*

To analyse EANTLI's ability to characterize intra-urban variability, we selected as examples Beijing, Shanghai, and Guangzhou, the three largest cities in China, which have the most serious NTL saturation problem. A parallel comparison of NTL, RCNTL, VIIRS, VANUI, and EANTLI was conducted by visualizing these indices for each city. The images were visualized using the 'percent clip' stretching method in the ArcGIS software (Figures 2–4). Vector maps of the PSA were overlaid on these images. Distinct land features (parks, CBDs, airports, etc.) were also labelled. As shown in Figures 2–4, the NTL images have the least variation in the PSAs, rendering detection of any land features impossible. The RCNTL images greatly reduce the saturation problem and the 'blooming' effect of NTL data. More spatial variation can be observed in the RCNTL images. However, it is still difficult to differentiate some of the selected land features. The VIIRS images show the most spatial variations among all the images. The saturation problem and the 'blooming' effect are both successfully solved, which makes it very easy to identify different land features in the VIIRS images. The VANUI introduces certain variations into the saturated NTL values, but the differences are not sufficiently significant, especially inside the PSAs. Certain land features can be easily differentiated from their surroundings, while others may be omitted. Meanwhile, the 'blooming' effect is still obvious in the VANUI images.

Generally, the EANTLI images look more similar to the VIIRS images than the RCNTL images or the VANUI images. Light saturation inside the PSAs is apparently

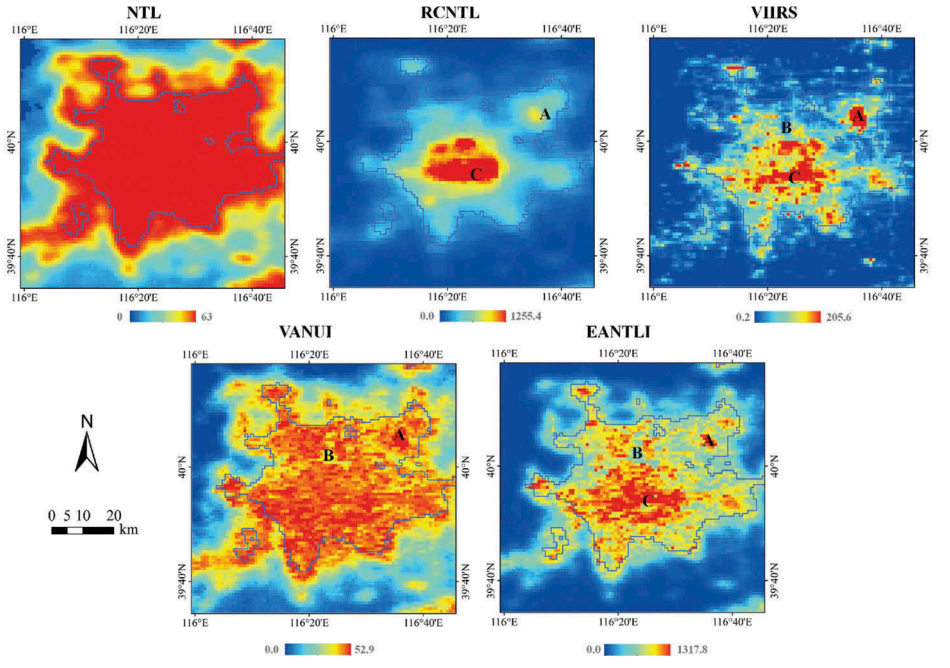

Figure 2. Comparison of NTL, RCNTL, VIIRS, VANUI, and EANTLI for Beijing. Identifiable land features include the Beijing Capital International Airport (A), the Olympic Forest Park (B), and Chang'an Street (C).

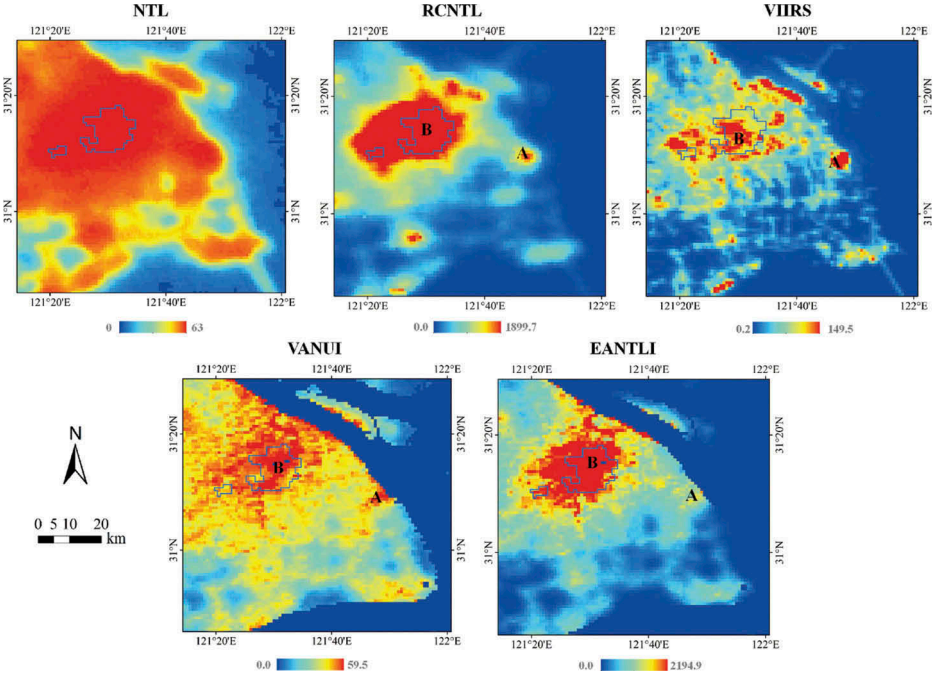

Figure 3. Comparison of NTL, RCNTL, VIIRS, VANUI, and EANTLI for Shanghai. Identifiable land features include the Shanghai Pudong International Airport (A) and the Lujiazui CBD (B).

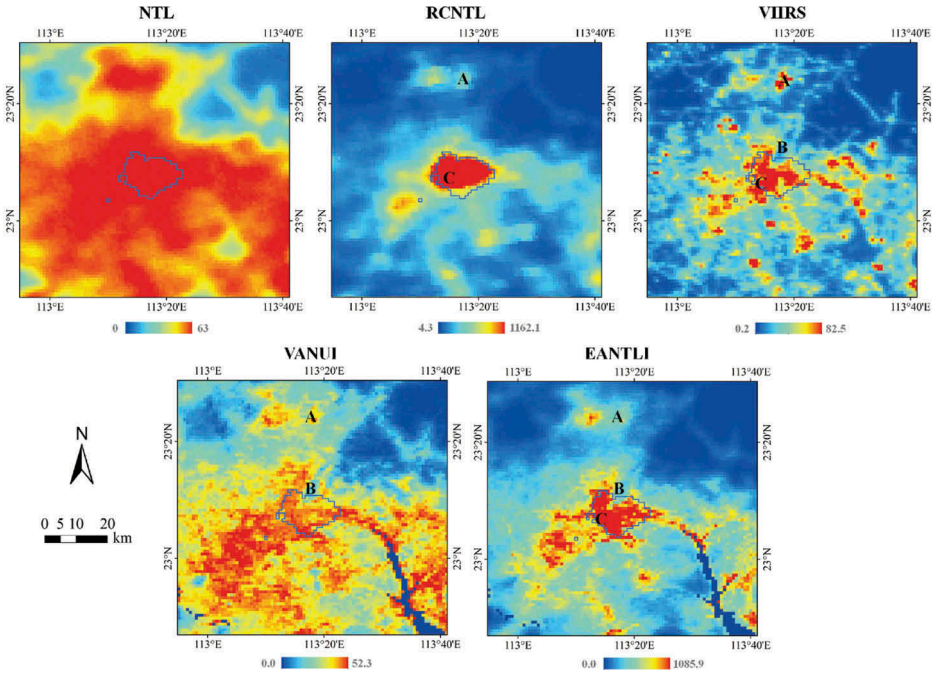

Figure 4. Comparison of NTL, RCNTL, VIIRS, VANUI, and EANTLI for Guangzhou. Identifiable land features include the Guangzhou Baiyun International Airport (A), Baiyun Mountain (B), and Guangzhou's Liwan CBD (C).

reduced in the EANTLI images, while the 'blooming' effect outside the PSAs is also noticeably mitigated. The EANTLI images show the second highest heterogeneity in the PSAs and the general spatial structures appear to be very similar to those of the VIIRS images. Differences among the selected land features are apparent. Parks, airports, and economic centres can be easily distinguished from their surrounding pixels.

To further examine EANTLI's performance, we calculated EANTLI and VANUI for 12 cities around the world and compared them with RCNTL and VIIRS (Figure 5). These cities vary greatly in terms of size, geography, climate, and economic base. As discussed in Zhang et al.'s study (2013), VANUI performs better in increasing the variability in intra-urban values for established cities, such as Los Angeles and Tokyo, compared with cities that have experienced significant growth over a relatively short time, such as Sao Paulo and Bengaluru. VANUI does not perform well in urban regions with an arid climate and low vegetation coverage, such as Phoenix. However, EANTLI consistently shows significant variation within these urban regions and noticeable mitigation of the 'blooming' effect outside the PSAs.

3.2. Latitudinal transect analysis

To further quantitatively verify the effectiveness of the proposed EANTLI, we compared the values of VANUI, EANTLI, RCNTL, and VIIRS along randomly selected latitudinal transects.

Figure 6 shows three latitudinal transects across the Jingjintang, Yangtze River delta, and Pearl River delta Urban Groups. Latitudes of these transects are 39° 50′ 42″ N,

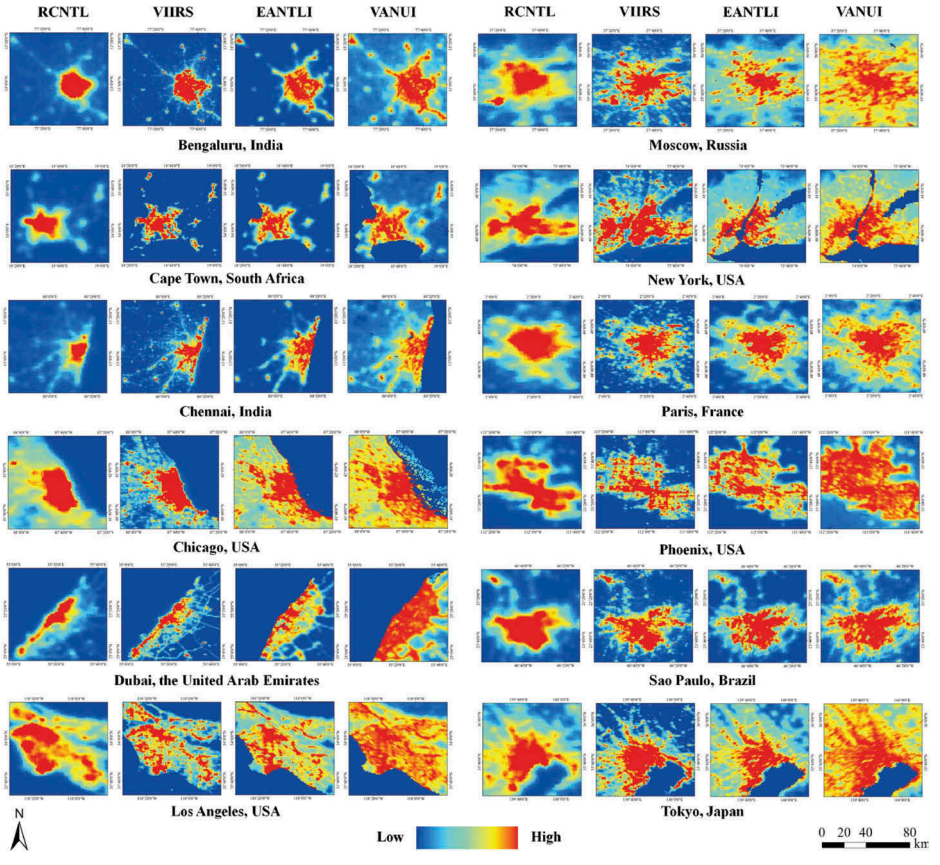

Figure 5. RCNTL, VIIRS, VANUI, and EANTLI for 12 cities around the world.

31° 7′ 40″ N, and 22° 46′ 28″ N, respectively. The values from the same transect are plotted in a line chart.

As shown in Figure 6, VANUI and EANTLI corrected the saturation in central urban areas. However, VANUI appears to overestimate lighting outside urban cores. In contrast, EANTLI's performance is substantially better. The shape of the EANTLI curves appears to be highly similar to the RCNTL and VIIRS curves. Most of the rises and falls of lighting are successfully captured by EANTLI.

We randomly selected 75 transects across the PSAs of the three Chinese urban groups and the 12 cities around the world as test samples to further compare the ability of EANTLI and VANUI to reduce saturation. Figure 7 shows the calculated VANUI and EANTLI along three transects of the Jingjintang, Yangtze River delta, and Pearl River delta Urban Groups against the RCNTL values in scatter plots. Linear regression models of VANUI–RCNTL and EANTLI–RCNTL as well as the determination coefficients (R^2) are plotted in Figure 7. The linear Pearson correlation coefficient (r) of the two vegetation-based urban indices and RCNTL/VIIRS of the 75 test samples are listed in Table 1.

Figure 7 shows that EANTLI has a stronger linear correlation with RCNTL than VANUI for the three transects. It can be noticed that a strong linear trend with only slight variation exists in the unsaturated NTL area (RCNTL values below 100), while for those located in the PSAs, a greater dispersion can be observed. Focusing on the PSA portion,

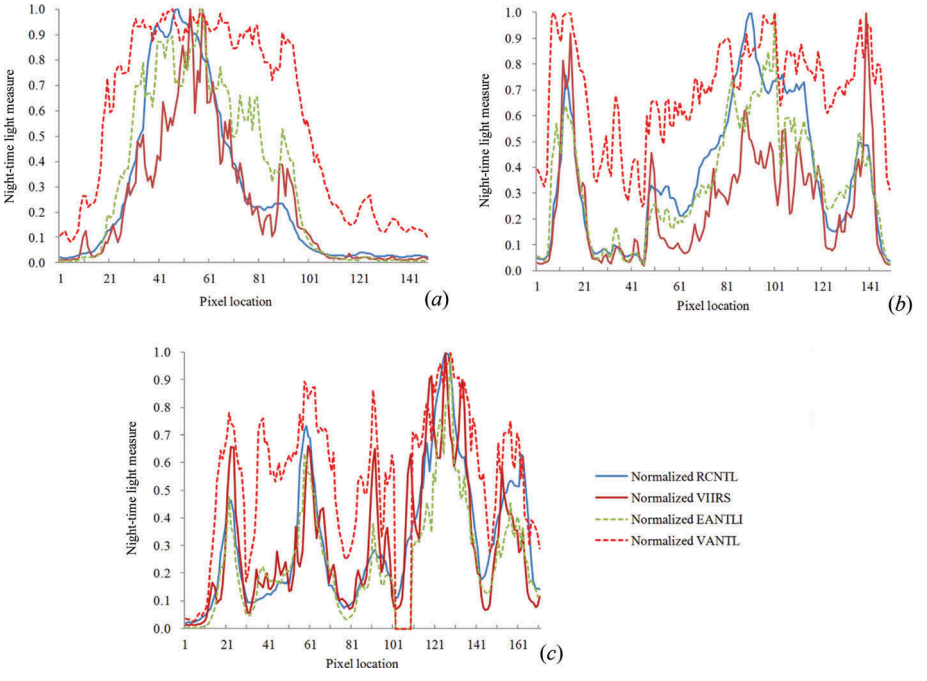

Figure 6. Latitudinal transects of VANUI, EANTLI, RCNTL, and VIIRS for (*a*) Jingjintang, (*b*) Yangtze River delta, and (*c*) Pearl River delta Urban Groups.

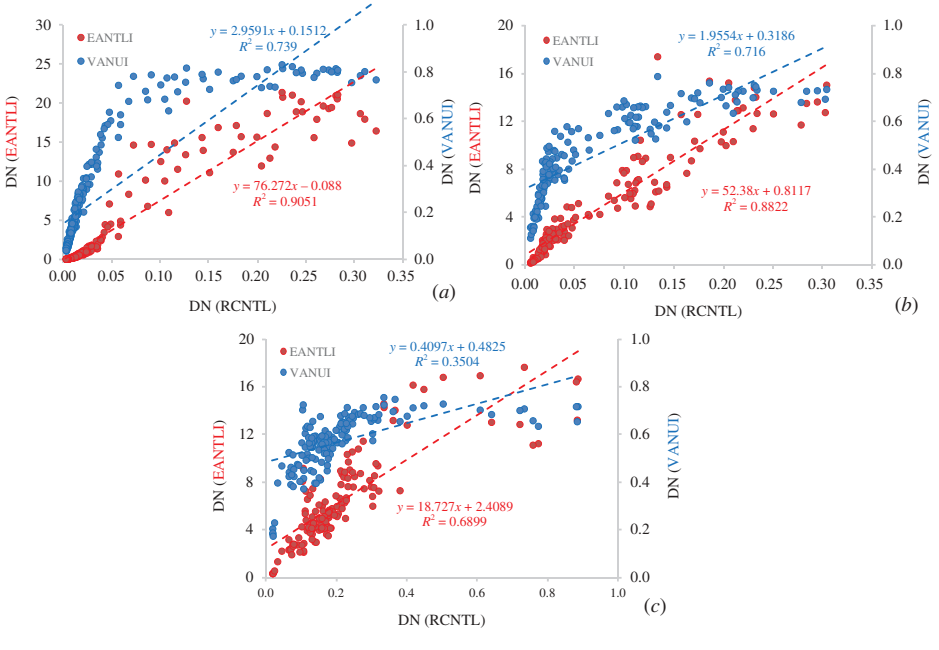

Figure 7. Relationships among VANUI, EANTLI, and RCNTL along the latitudinal transects of the (*a*) Jingjintang, (*b*) Yangtze River delta, and (*c*) Pearl River delta Urban Groups.

Table 1. Linear correlation (r) among EANTLI, VANUI, RCNTL, and VIIRS.

City	EANTLI–RCNTL	VANUI–RCNTL	EANTLI–VIIRS	VANUI–VIIRS
Beijing	0.90	0.76	0.85	0.74
Shanghai	0.90	0.69	0.83	0.77
Guangzhou	0.90	0.76	0.87	0.80
New York	0.80	0.85	0.79	0.79
Los Angeles	0.80	0.77	0.69	0.64
Chicago	0.89	0.81	0.83	0.73
Phoenix	0.89	0.83	0.80	0.73
Tokyo	0.87	0.84	0.91	0.83
Moscow	0.89	0.78	0.86	0.74
Paris	0.95	0.92	0.94	0.89
Capetown	0.96	0.93	0.90	0.85
Dubai	0.79	0.62	0.71	0.57
Sao Paulo	0.92	0.89	0.86	0.86
Bengaluru	0.91	0.82	0.84	0.76
Chennai	0.91	0.83	0.85	0.76
Average	**0.88**	**0.81**	**0.84**	**0.76**

the linear correlation is poor for EANTLI and VANUI. This result is expected because the values of EANTLI and VANUI outside the PSAs are primarily determined by NTL, which has a good linear relationship with RCNTL. Inside the PSAs, the EANTLI and VANUI values are only varied by the vegetation index because of the saturation of NTL. Figure 7 also shows that EANTLI introduces greater variation inside the PSAs, and the EANTLI data points are more coherent.

Table 1 shows that EANTLI has a stronger linear correlation with RCNTL and VIIRS. Except for New York City, EANTLI has a better performance than VANUI in 14 other cities. The average linear Pearson correlation coefficient of EANTLI and RCNTL is 0.88 compared with a value of 0.81 for VANUI; when VIIRS is used as a reference, the result is 0.84 *versus* 0.76, respectively. EANTLI still outperforms VANUI.

3.3. *Electric power consumption estimation*

These analyses proved EANTLI's ability to reduce saturation in PSA and increase the similarity to RCNTL and VIIRS. Because NTL data have been widely used as proxies for human settlements, we also tested the performance of EANTLI in these applications. Elvidge et al. (1999) have proved that an RCNTL image could be used to accurately estimate electric power consumption. Inspired by this study, we calculated cumulative DN values of RCNTL, VANTL, and EANTLI in 2010 for 166 Chinese prefecture-level cities and analysed their linear correlation with the electric power consumption of these cities. China is usually divided into three parts, west, central, and east, based on economic development and geography. Provinces in the eastern part are mostly coastally located and economically developed, while provinces in the middle and western parts are inland located and less developed. Considering that electric power consumption patterns vary in different stages of development, we divided the 166 cities correspondingly into three groups, namely eastern, middle, and western groups. For each group, cumulative DN values of RCNTL, VANTL, and EANTLI are plotted against the total electric power consumption of cities in that group (Figure 8).

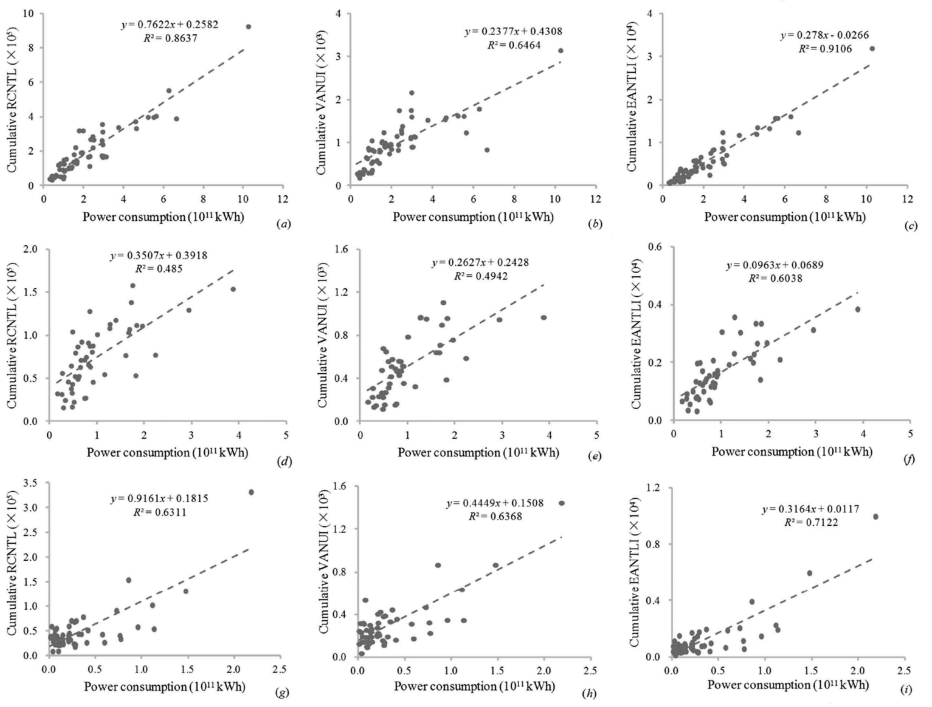

Figure 8. Electric power consumption estimation of 166 Chinese prefecture-level cities in eastern (parts (*a*), (*b*), and (*c*)), middle (parts (*d*), (*e*), and (*f*)), and western (parts (*g*), (*h*), and (*i*)) groups based on cumulative RCNTL (parts (*a*), (*d*), and (*g*)), VANTL (parts (*b*), (*e*), and (*h*)), and EANTLI (parts (*c*), (*f*), and (*i*)).

As Figure 8 shows, EANTLI has the highest R^2 of the three groups, indicating that EANTLI performs best in the estimation of electric power consumption for the 166 cities in China. Note that EANTLI consistently outperforms the non-saturated RCNTL, while VANTL shows only a slightly better performance than RCNTL. These results indicate that EANTLI has great potential for applications in quantitative studies that use NTL as proxy of urban settlements or human activities.

4. Discussion

In the application of VANUI, the simple expression '(1 – (NDVI))' is used as the adjustment factor for NTL. Although the index can characterize intra-urban variability in night-time luminosity, it indiscriminately reduces all of the NTL values, while the visible and near-infrared radiances inside the PSAs are actually greater than the radiances recorded by DMSP-OLS. In addition, NDVI itself suffers from saturation problems. Therefore, we used EVI to construct a new index, which increases NTL DN values in the urban cores and minimizes them in the suburbs, to achieve results that are more realistic.

The results of the three experiments prove that EANTLI successfully solved the mentioned problems. The heterogeneity inside the PSAs is increased, and saturation is greatly reduced. In addition, the blooming effect is mitigated. The spatial distribution of

EANTLI is similar to those of RCNTL and VIIRS. Randomly selected latitudinal transects proved that EANTLI can capture peaks and valleys of the non-saturated RCNTL and VIIRS. In the estimation of electric power consumption, EANTLI achieved the most accurate results, which were even superior to those of RCNTL.

Despite these advantages, EANTLI still has limitations. First, for areas with low EVI and high NTL, e.g. large docks or plazas, the EANTLI value will be exceptionally high because the adjustment factor k is expressed as '(2/(EVI) – 1)' inside the PSAs. Due to the coarse spatial resolution, the MODIS EVI product has serious mixed pixel problems around waterbodies where EVI values are below or close to 0. Although we have set a threshold of 0.01 to remove some of these mixed pixels in our calculation, the results are still not ideal. EANTLI's failure to outperform VANUI in New York City is just caused by the existence of many mixed pixels along the Hudson River. Second, the removal of pixels with negative and extremely low EVI values may result in unrealistic light 'fault zones'. These problems may be solved by introducing a proper application strategy, for example, using dynamic EVI threshold values and applying cubic convolution along the 'fault zones'.

With its similarity to the non-saturated RCNTL and VIIRS data, EANTLI has great potential for many applications. For example, EANTLI can be used to extract more accurate urban borders and urban areas because it can mitigate the 'blooming' effect. Better estimation of socio-economic parameters and populations may also be achieved for years without RCNTL data. Since long time series of DMSP-OLS NTL and MODIS EVI products are both available, it is possible to develop an EANTLI time-series data set. Based on such a data set, the temporal dynamics of socio-economic and demographic changes, such as urban expansion, economic growth, temporal–spatial distribution of population, etc., could be better analysed. Tracking of the multi-year night-time light change in urban centres could also be realized.

5. Conclusions

In this study, we proposed an EVI-adjusted NTL index, namely EANTLI. The index is a further development of the VANUI. Both of the indices are based on the inverse correlation between vegetation and urban night-time light. However, EANTLI is designed to enlarge NTL when the normalized NTL is greater than EVI and to reduce NTL when the normalized NTL is less than EVI. Therefore, NTL saturation in a PSA is reduced, and light intensity differences between urban centres and suburban regions are enhanced.

To evaluate EANTLI's effectiveness, we compared its spatial distribution in 15 cities around the world with VANUI, as well as with the RCNTL and the new VIIRS data. The visual results show that EANTLI can reveal substantially better spatial details in urban cores compared with VANUI and RCNTL, while the details are slightly inferior to those provided by VIIRS. Quantitative experiments of randomly selected latitudinal transects across the 15 world cities revealed that EANTLI is closer to RCNTL and VIIRS compared with VANUI, while the linear correlation between EANTLI and RCNTL has a coefficient of 0.88, which is higher than the value of 0.81 for VANUI. Finally, we illustrated that EANTLI provided better evaluation of electric power consumption of 166 Chinese prefecture-level cities.

In conclusion, EANTLI can effectively reduce the NTL saturation problem and increase the heterogeneity in urban and suburban regions. The spatial distribution of EANTLI closely resembles that of RCNTL and VIIRS; therefore, it can be used as an

ideal substitution to evaluate urban settlements and human activities in urban areas. Further studies will be focused on EANTLI's applications in other fields, such as population density simulation and socio-economic activity estimation.

Disclosure statement

No potential conflict of interest was reported by the authors.

Funding

This work was supported by the National Natural Science Foundation of China [grant number 41371499]; and the startup fund for Prof. Liu Lin from the One Thousand Talents Program of Sun Yat-sen University.

References

Amaral, S., G. Câmara, A. M. V. Monteiro, J. A. Quintanilha, and C. D. Elvidge. 2005. "Estimating Population and Energy Consumption in Brazilian Amazonia Using DMSP Night-Time Satellite Data." *Computers, Environment and Urban Systems* 29: 179–195. doi:10.1016/j.compenvurbsys.2003.09.004.

Amaral, S., A. M. V. Monteiro, G. Camara, and J. A. Quintanilha. 2006. "DMSP/OLS Night-Time Light Imagery for Urban Population Estimates in the Brazilian Amazon." *International Journal of Remote Sensing* 27: 855–870. doi:10.1080/01431160500181861.

Baugh, K., F. C. Hsu, C. D. Elvidge, and M. Zhizhin. 2013. "Nighttime Lights Compositing Using the VIIRS Day-Night Band: Preliminary Results." *Proceedings of the Asia Pacific Advanced Network* 35: 70–86. doi:10.7125/APAN.35.8.

Chalkias, C., M. Petrakis, B. Psiloglou, and M. Lianou. 2006. "Modelling of Light Pollution in Suburban Areas Using Remotely Sensed Imagery and GIS." *Journal of Environmental Management* 79: 57–63. doi:10.1016/j.jenvman.2005.05.015.

Chand, T. K., K. Badarinath, C. D. Elvidge, and B. T. Tuttle. 2009. "Spatial Characterization of Electrical Power Consumption Patterns over India Using Temporal DMSP-OLS Night-Time Satellite Data." *International Journal of Remote Sensing* 30: 647–661. doi:10.1080/01431160802345685.

Chen, X., and W. D. Nordhaus. 2011. "Using Luminosity Data as a Proxy for Economic Statistics." *Proceedings of the National Academy of Sciences* 108: 8589–8594. doi:10.1073/pnas.1017031108.

Doll, C. H., J. Muller, and C. D. Elvidge. 2000. "Night-Time Imagery as a Tool for Global Mapping of Socioeconomic Parameters and Greenhouse Gas Emissions." *AMBIO* 29: 157–162. doi:10.1579/0044-7447-29.3.157.

Elvidge, C. D., K. E. Baugh, S. J. Anderson, P. C. Sutton, and T. Ghosh. 2012. "The Night Light Development Index (NLDI): A Spatially Explicit Measure of Human Development from Satellite Data." *Social Geography* 7: 23–35. doi:10.5194/sg-7-23-2012.

Elvidge, C. D., K. E. Baugh, J. B. Dietz, T. Bland, P. C. Sutton, and H. W. Kroehl. 1999. "Radiance Calibration of DMSP-OLS Low-Light Imaging Data of Human Settlements." *Remote Sensing of Environment* 68: 77–88. doi:10.1016/S0034-4257(98)00098-4.

Elvidge, C. D., K. E. Baugh, E. A. Kihn, H. W. Kroehl, E. R. Davis, and C. W. Davis. 1997. "Relation between Satellite Observed Visible-Near Infrared Emissions, Population, Economic Activity and Electric Power Consumption." *International Journal of Remote Sensing* 18: 1373–1379. doi:10.1080/014311697218485.

Elvidge, C. D., P. Cinzano, D. R. Pettit, J. Arvesen, P. Sutton, C. Small, R. Nemani, T. Longcore, C. Rich, J. Safran, J. Weeks, and S. Ebener. 2007. "The Nightsat Mission Concept." *International Journal of Remote Sensing* 28: 2645–2670. doi:10.1080/01431160600981525.

Elvidge, C. D., M. Zhizhin, F. C. Hsu, and K. E. Baugh. 2013. "VIIRS Nightfire: Satellite Pyrometry at Night." *Remote Sensing* 5: 4423–4449. doi:10.3390/rs5094423.

Ghosh, T., R. L. Powell, C. D. Elvidge, K. E. Baugh, P. C. Sutton, and S. Anderson. 2010. "Shedding Light on the Global Distribution of Economic Activity." *The Open Geography Journal* 3: 148–161.

He, C., Q. Ma, T. Li, Y. Yang, and Z. Liu. 2012. "Spatiotemporal Dynamics of Electric Power Consumption in Chinese Mainland from 1995 to 2008 Modeled Using DMSP/OLS Stable Nighttime Lights Data." *Journal of Geographical Sciences* 22: 125–136. doi:10.1007/s11442-012-0916-3.

Henderson, J. V., A. Storeygard, and D. N. Weil. 2012. "Measuring Economic Growth from Outer Space." *American Economic Review* 102: 994–1028. doi:10.1257/aer.102.2.994.

Hillger, D., T. Kopp, T. Lee, D. Lindsey, C. Seaman, S. Miller, J. Solbrig, S. Kidder, S. Bachmeier, and T. Jasmin, et al.. 2013. "First-Light Imagery from Suomi NPP VIIRS." *Bulletin of the American Meteorological Society* 94: 1019–1029. doi:10.1175/BAMS-D-12-00097.1.

Huete, A., K. Didan, T. Miura, E. P. Rodriguez, X. Gao, and L. G. Ferreira. 2002. "Overview of the Radiometric and Biophysical Performance of the MODIS Vegetation Indices." *Remote Sensing of Environment* 83: 195–213. doi:10.1016/S0034-4257(02)00096-2.

Huete, A. R., C. O. Justice, and W. Van Leeuwen. 1999. *MODIS Vegetation Index (MOD 13). Version 3. Algorithm Theoretical Basis Document*. Greenbelt, MD: NASA, Goddard Space Flight Center. Accessed May 7, 2011.

Imhoff, M. L., L. Bounoua, R. DeFries, W. T. Lawrence, D. Stutzer, C. J. Tucker, and T. Ricketts. 2004. "The Consequences of Urban Land Transformation on Net Primary Productivity in the United States." *Remote Sensing of Environment* 89: 434–443. doi:10.1016/j.rse.2003.10.015.

Imhoff, M. L., C. J. Tucker, W. T. Lawrence, and D. C. Stutzer. 2000. "The Use of Multisource Satellite and Geospatial Data to Study the Effect of Urbanization on Primary Productivity in the United States." *IEEE Transactions on Geoscience and Remote Sensing* 38: 2549–2556. doi:10.1109/36.885202.

Letu, H., M. Hara, G. Tana, and F. Nishio. 2012. "A Saturated Light Correction Method for DMSP/OLS Nighttime Satellite Imagery." *IEEE Transactions on Geoscience and Remote Sensing* 50: 389–396. doi:10.1109/TGRS.2011.2178031.

Letu, H., T. Y. Nakajima, and F. Nishio. 2014. "Regional-Scale Estimation of Electric Power and Power Plant CO_2 Emissions Using Defence Meteorological Satellite Program Operational Linescan System Nighttime Satellite Data." *Environmental Science & Technology Letters* 1: 259–265. doi:10.1021/ez500093s.

Li, X., H. Xu, X. Chen, and C. Li. 2013. "Potential of NPP-VIIRS Nighttime Light Imagery for Modelling the Regional Economy of China." *Remote Sensing* 5: 3057–3081. doi:10.3390/rs5063057.

Liu, H., and A. R. Huete. 1995. "A Feedback Based Modification of the NDVI to Minimize Canopy Background and Atmospheric Noise." *IEEE Transactions on Geoscience and Remote Sensing* 33: 457–465. doi:10.1109/36.377946.

Lo, C. P. 2001. "Modeling the Population of China Using DMSP Operational Linescan System Nighttime Data." *Photogrammetric Engineering and Remote Sensing* 67: 1037–1047.

Lo, C. P. 2002. "Urban Indicators of China from Radiance-Calibrated Digital DMSP-OLS Nighttime Images." *Annals of the Association of American Geographers* 92: 225–240. doi:10.1111/1467-8306.00288.

Ma, T., C. Zhou, T. Pei, S. Haynie, and J. Fan. 2012. "Quantitative Estimation of Urbanization Dynamics Using Time Series of DMSP/OLS Nighttime Light Data: A Comparative Case Study from China's Cities." *Remote Sensing of Environment* 124: 99–107. doi:10.1016/j.rse.2012.04.018.

Miller, S. D., S. P. Mills, C. D. Elvidge, D. T. Lindsey, T. F. Lee, and J. D. Hawkins. 2012. "Suomi Satellite Brings to Light a Unique Frontier of Nighttime Environmental Sensing Capabilities." *Proceedings of the National Academy of Sciences of the USA* 109: 15706–15711. doi:10.1073/pnas.1207034109.

Pandey, B., P. K. Joshi, and K. C. Seto. 2013. "Monitoring Urbanization Dynamics in India Using DMSP/OLS Night Time Lights and SPOT-VGT Data." *International Journal of Applied Earth Observation and Geoinformation* 23: 49–61. doi:10.1016/j.jag.2012.11.005.

Raupach, M. R., P. J. Rayner, and M. Paget. 2010. "Regional Variations in Spatial Structure of Nightlights, Population Density and Fossil-Fuel CO2 Emissions." *Energy Policy* 38: 4756–4764. doi:10.1016/j.enpol.2009.08.021.

Shi, K., B. Yu, Y. Huang, Y. Hu, B. Yin, Z. Chen, L. Chen, and J. Wu. 2014. "Evaluating the Ability of NPP-VIIRS Nighttime Light Data to Estimate the Gross Domestic Product and the Electric

Power Consumption of China at Multiple Scales: A Comparison with DMSP-OLS Data." *Remote Sensing* 6: 1705–1724. doi:10.3390/rs6021705.

Sutton, P. C. 2003. "A Scale-Adjusted Measure of 'Urban Sprawl' Using Nighttime Satellite Imagery." *Remote Sensing of Environment* 86: 353–369. doi:10.1016/S0034-4257(03)00078-6.

Sutton, P. C., C. D. Elvidge, and T. Ghosh. 2007. "Estimation of Gross Domestic Product at Sub-National Scales Using Nighttime Satellite Imagery." *International Journal of Ecological Economics & Statistics* 8: 5–21.

Wei, Y., H. Liu, W. Song, B. Yu, and C. Xiu. 2014. "Normalization of Time Series DMSP-OLS Nighttime Light Images for Urban Growth Analysis with Pseudo Invariant Features." *Landscape and Urban Planning* 128: 1–13. doi:10.1016/j.landurbplan.2014.04.015.

Yu, B., K. Shi, Y. Hu, C. Huang, Z. Chen, and J. Wu. 2015. "Poverty Evaluation Using NPP-VIIRS Nighttime Light Composite Data at the County Level in China." *IEEE Journal of Selected Topics in Applied Earth Observations and Remote Sensing* 8: 1217–1229.

Zeng, C., Y. Zhou, S. Wang, F. Yan, and Q. Zhao. 2011. "Population Spatialization in China Based on Night-Time Imagery and Land Use Data." *International Journal of Remote Sensing* 32: 9599–9620. doi:10.1080/01431161.2011.569581.

Zhang, Q., C. Schaaf, and K. C. Seto. 2013. "The Vegetation Adjusted NTL Urban Index: A New Approach to Reduce Saturation and Increase Variation in Nighttime Luminosity." *Remote Sensing of Environment* 129: 32–41. doi:10.1016/j.rse.2012.10.022.

Zhang, Q., and K. C. Seto. 2011. "Mapping Urbanization Dynamics at Regional and Global Scales Using Multi-Temporal DMSP/OLS Nighttime Light Data." *Remote Sensing of Environment* 115: 2320–2329. doi:10.1016/j.rse.2011.04.032.

Zhuo, L., T. Ichinose, J. Zheng, J. Chen, P. J. Shi, and X. Li. 2009. "Modelling the Population Density of China at the Pixel Level Based on DMSP/OLS Non-Radiance-Calibrated Night-Time Light Images." *International Journal of Remote Sensing* 30: 1003–1018. doi:10.1080/01431160802430693.

Ziskin, D., K. Baugh, and F. C. Hsu. 2010. "Methods Used for the 2006 Radiance Lights." *Proceedings of the Asia Pacific Advanced Network* 30: 131–142.